

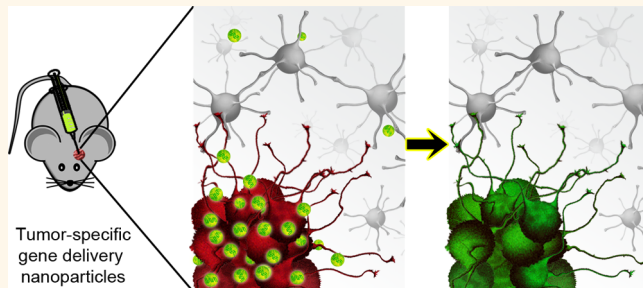


Biodegradable Polymeric Nanoparticles Show High Efficacy and Specificity at DNA Delivery to Human Glioblastoma *in Vitro* and *in Vivo*

Hugo Guerrero-Cázares,^{†,#} Stephany Y. Tzeng,^{‡,§,#} Noah P. Young,^{‡,§} Ameer O. Abutaleb,[†] Alfredo Quiñones-Hinojosa,^{†,||,*} and Jordan J. Green^{†,‡,§,||,¶,*}

[†]Department of Neurosurgery, [‡]Department of Biomedical Engineering, [§]Translational Tissue Engineering Center, ^{||}Institute for Nanobiotechnology, and [¶]Department of Ophthalmology, Johns Hopkins University School of Medicine, 400 North Broadway, Baltimore, Maryland 21231, United States. [#]These authors contributed equally.

ABSTRACT Current glioblastoma therapies are insufficient to prevent tumor recurrence and eventual death. Here, we describe a method to treat malignant glioma by nonviral DNA delivery using biodegradable poly(β-amino ester)s (PBAEs), with a focus on the brain tumor initiating cells (BTICs), the tumor cell population believed to be responsible for the formation of new tumors and resistance to many conventional therapies. We show transfection efficacy of >60% and low biomaterial-mediated cytotoxicity in primary human BTICs *in vitro* even when the BTICs are grown as 3-D oncospheres. Intriguingly, we find that these polymeric nanoparticles show intrinsic specificity for nonviral transfection of primary human BTICs over primary healthy human neural progenitor cells and that this specificity is not due to differences in cellular growth rate or total cellular uptake of nanoparticles. Moreover, we demonstrate that biodegradable PBAE/DNA nanoparticles can be fabricated, lyophilized, and then stored for at least 2 years without losing efficacy, increasing the translational relevance of this technology. Using lyophilized nanoparticles, we show transgene expression by tumor cells after intratumoral injection into an orthotopic murine model of human glioblastoma. PBAE/DNA nanoparticles were more effective than naked DNA at exogenous gene expression *in vivo*, and tumor cells were transfected more effectively than noninvaded brain parenchyma *in vivo*. This work shows the potential of nonviral gene delivery tools to target human brain tumors.



KEYWORDS: glioblastoma · nonviral gene delivery · nanomedicine · targeted delivery

Brain tumors affect over 600000 patients in the United States, with glioblastoma (GBM) being the most common form of primary brain tumor in adults¹ and considered the most lethal and aggressive form of brain cancer. Nearly 25000 new cases of brain cancer are diagnosed in the United States each year, accounting for nearly 15000 deaths.^{2–4} Patients who suffer from GBM have a median survival of 14.6 months despite surgery, radiation, and chemotherapy combined.^{2,5–7} This devastating prognosis for a GBM patient has not significantly changed for the past decades, which underlines the important necessity of developing new alternative therapies. One potential strategy for improving GBM patient outcomes is the incorporation of therapeutic

genes in patients with brain tumors. Gene therapy can induce the expression of genes that induce apoptosis if expressed by tumor cells, are neuroprotective if expressed by the noncancerous tissue, or modulate immune responses to the tumor.^{8–13} However, most common gene therapy approaches involve the use of viral vectors, which are characterized by several safety concerns that limit their translational potential.¹⁴ Viral vectors often show insufficient gene delivery efficacy *in vivo* and are immunogenic, preventing effective initial infection as well as repeated administration.¹⁵ For example, a study using adenovirus-mediated suicide gene delivery in a primate model for glioma found that the dosage of viral particles was limited by toxicity and the development of

* Address correspondence to aquinon2@jhmi.edu, green@jhu.edu.

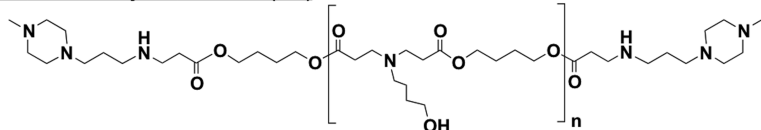
Received for review February 28, 2014 and accepted April 26, 2014.

Published online April 26, 2014
10.1021/nn501197v

© 2014 American Chemical Society

Chart 1. Monomers used in PBAE synthesis^aMonomers

B3b		1,3-butanediol diacrylate	E1		propane-1,3-diamine
B4		1,4-butanediol diacrylate	E3		pentane-1,3-diamine
B5		1,5-pentanediol diacrylate	E4		2-methylpentane-1,5-diamine
B6		1,6-hexanediol diacrylate	E5		1,11-diamino-3,6,9-trioxaundecane
S3		3-amino-1-propanol	E6		2-(3-aminopropyl)aminoethanol
S4		4-amino-1-butanol	E7		1-(3-aminopropyl)-4-methylpiperazine
S5		5-amino-1-pentanol	E8		1-(3-aminopropyl)pyrrolidine
			E10		cystamine

Representative Polymer: B4-S4-E7 (447)

^a One backbone (B) monomer is polymerized with one side chain (S). This base polymer is then end-capped with a small molecule (E).

humoral immune response.¹⁶ In some cases, viral gene therapy has been implemented in GBM patients without showing increased adverse side effects; however, in many cases, the prognosis has not been improved due to poor delivery of the therapeutic agents, including in a phase III clinical trial.¹⁷

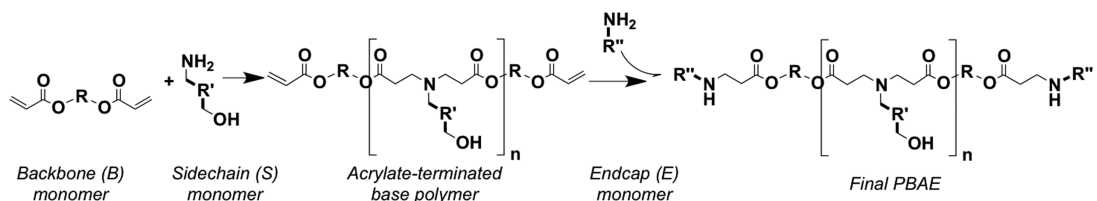
Nonviral gene delivery strategies include utilizing biomaterials such as lipids, polymers, peptides, sugars, dendrimers, and other materials that are capable of binding or encapsulating nucleic acids and then facilitating intracellular delivery through multiple delivery steps.^{18–20} We have developed a polymer library by varying the different structural components that make up a class of cationic linear polymers, poly(β -amino ester)s, by systematically tuning the polymer backbone, side chain, polymer terminal group, and degradable linkages that compose the polymers.^{21–23} These cationic polymers self-assemble with DNA to form nanoparticles that encapsulate up to 100 plasmids per nanoparticle,²⁴ are noncytotoxic and biodegradable with a half-life between 1 and 7 h in aqueous conditions,²⁵ and show promise for therapeutic use.²⁶

While DNA delivery has been studied in various research settings, nonviral *in vivo* and clinically translatable technologies must be further developed to enhance efficacy, safety, and specificity. To promote tumor targeting of nonviral nucleic acid delivery

nanoparticles, strategies such as addition of a targeting ligand to the nanoparticle²⁷ or transcriptional control through plasmid promoter design²⁸ have been previously utilized. In this study, we explored the ability of biomaterial-mediated intrinsic targeting of primary human brain cancer cells over primary human neural progenitor cells without the use of a targeting ligand or transcriptional targeting. We show effective nonviral DNA delivery to human primary brain tumor initiating cells (BTICs), thought to contribute to tumor initiation and recurrence. The nonviral nanoparticles used were formulated for long-term stability and functioned in an orthotopic murine model of GBM, showing efficacy in targeting cancer cells while sparing the noncancer tissue.

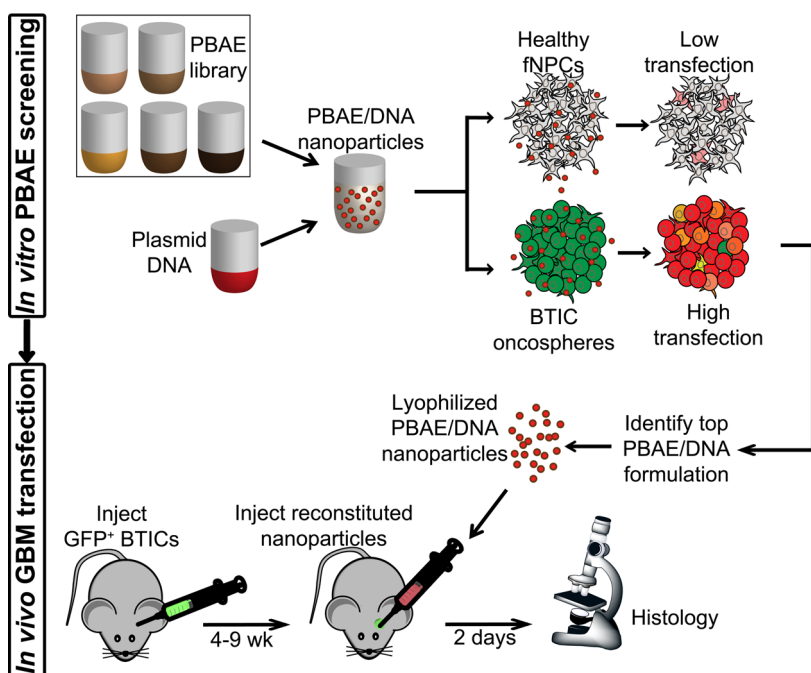
RESULTS

Safe and Effective Transfection of Brain Tumor Initiating Cells (BTIC) as 3-D Oncospheres. Poly(β -amino ester)s (PBAEs) were synthesized as previously described²⁹ using the monomers defined in Chart 1 and the reaction scheme shown in Scheme 1. Polymers were then named according to the backbone, side-chain, and end-cap monomers used in synthesis, with the synthesis ratio of backbone to side-chain monomer indicated (e.g., B4 polymerized with S5 at 1.2:1 ratio and end-capped with E3 is called “453, 1.2:1”).



Scheme 1. PBAE synthesis reaction scheme.

Scheme 2. *In vitro* and *in vivo* DNA delivery scheme^a



^a A library of PBAEs is evaluated for DNA delivery efficacy in brain tumor initiating cells (BTICs) and low efficacy in fetal neural progenitor cells (fNPCs). The top formulation was used to deliver a fluorescence gene to tumor cells in a mouse model of GBM.

Nanoparticles were composed of varying ratios of polymer mass to DNA mass (w/w). We evaluated the transfection efficacy and safety of PBAE/DNA nanoparticles on primary cultures of human BTIC cells maintained as 3-D oncospheres, as depicted in Scheme 2. BTIC sample JHGBM-551 oncospheres were transfected with PBAEs complexed with DsRed-encoding DNA. Transfection efficacy and viability (lack of cytotoxicity) were measured using high-throughput flow cytometry and the MTS assay (Figure 1). As we have recently observed,^{21,22} we found that increased hydrophobicity (estimated by the number of carbons in the polymer's repeat unit) correlated with increased transfection efficacy as well as increased toxicity; in addition, the end-caps designated E3, E6, and E7 in Scheme 1 were generally the most effective. Leading polymers from this initial screening with 8–9 carbon repeat units were resynthesized and purified with ether to remove unreacted amine monomer (marked by the letter “e”, such as “453e”) for a second evaluation on BTIC oncospheres. Five polymers in this screen with

low cytotoxicity and high transfection efficacy were identified, with leading polymer, 447e, and other formulations yielding >80% viability. Fluorescence microscopy and flow cytometry showed >50% of cells in the oncospheres expressing the DsRed transgene when transfected with the top PBAE formulations (Figure 2). This work demonstrates for the first time that PBAE polymeric nanoparticles can significantly transfect 3-D oncospheres throughout the oncospheres volume, rather than only transfecting cells at the surface as with 2-D cell culture.

PBAE/DNA Nanoparticles Are Effective in Btcs from Multiple Patient Sources. The purified polymers were evaluated on a second sample of primary cultured BTICs derived from a different patient (JHGBM-276), using GFP DNA as a transfection marker (Figure S1, Supporting Information). Similarly high transfection efficacy was seen in JHGBM-276 BTICs, with PBAE 447e once again a leading polymer ($61 \pm 3\%$ transfection with $97 \pm 7\%$ viability). However, PBAE 537e was found to be the top formulation for transfection of JHGBM-276 BTICs, with

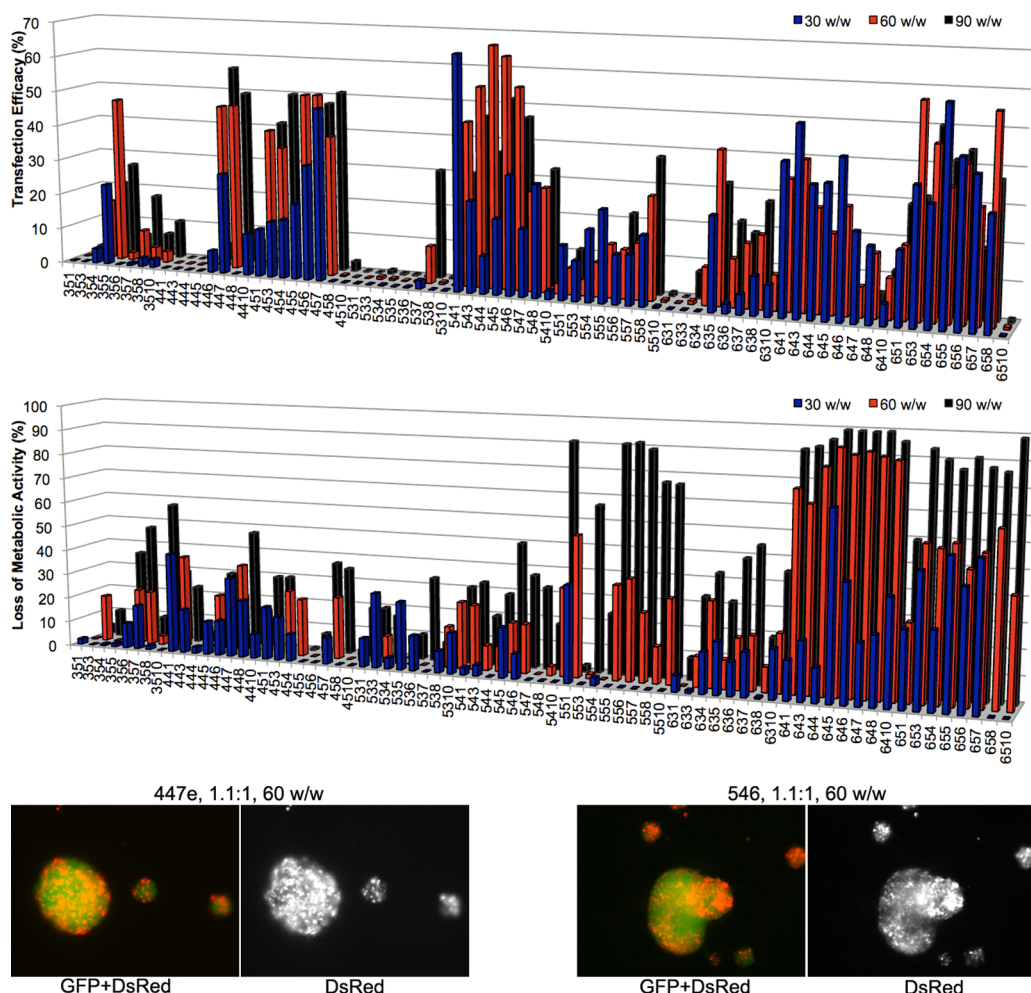


Figure 1. Evaluation of PBAEs for oncosphere transfection efficacy and safety. A wide screen of PBAE formulations, including different PBAE chemical structures and polymer/DNA ratios (w/w), was used to transfect 3-D BTIC JHGBM-551 oncospheres. All PBAEs used here (x-axis) were synthesized at a 1.2:1 B:S ratio. Leading polymers from this screen were chosen on the basis of high transfection efficacy (percent of cells transfected) and low toxicity (loss of relative metabolic activity). Fluorescence microscopy shows GFP⁺ oncospheres transfected with DsRed using purified PBAEs.

up to $76 \pm 2\%$ transfection with $90 \pm 4\%$ viability, although it transfected only between 20 and 45% of cells in JHGBM-551 BTICs. A moderate correlation in transfection efficacy of PBAE formulations ($r^2 = 0.42$) was found between two oncosphere cultures (JHGBM-551 and JHGBM-276), with 537e as the only statistical outlier. Outlier statistics calculations were done using Prism software (see the Methods). The non-537e polymers show a stronger correlation between the two primary glioblastoma oncospheres cultures ($r^2 = 0.66$) (Figure 3). A strong correlation was also found between transfection of oncospheres and monolayer cultures ($r^2 = 0.79$), indicating that, while a few polymers like 537e may have some specificity for one human cell sample over another, trends in transfection found in one GBM cell sample are largely applicable to other GBM samples, even when derived from separate patient sources.

Nanoparticle Transfection Efficacy Is Specific for Human Brain Tumor Initiating Cells over Human Neural Progenitor Cells. Our previous work suggested that an optimized PBAE nanoparticle formulation could be more effective at

transferring one patient-derived BTIC culture, JHGBM-551, than one fNPC culture, F34.²⁹ These observations were significantly strengthened by evaluating additional PBAE nanoparticle formulations in multiple patient-derived BTIC cultures and multiple fNPC cultures. Here, our top polymeric nanoparticle was tested on four patient-derived BTIC cultures (JHGBM-276, JHGBM-551, JHGBM-854, and JHGBM-965) as well as on three healthy, noncancerous primary human fetal neural progenitor cell cultures (fNPCs) (F34, F54, and F48) cultured in the same conditions as their cancer counterparts. We first evaluated PBAEs in JHGBM-276 BTICs and F34 fNPCs (Figure 4A), which showed that many of the PBAEs had significantly higher transfection in BTICs compared to fNPCs. We further evaluated our top PBAE, 447e, on the four BTIC and three fNPC cultures using two PBAE/DNA ratios (30 w/w and 60 w/w) and a range of nanoparticle doses. When results of transfection were combined for all BTIC and fNPC cells, at every dose tested, significantly higher expression was seen in BTICs over fNPCs (Figure 4B,C).

Of note, the difference between BTIC and fNPC transfections was even more striking when measured by intensity of GFP fluorescence from the cell population, indicating that several times more protein was being produced by transfected BTICs compared to

transfected fNPCs. This was particularly evident at lower doses, for which fNPCs were transfected very poorly or not at all, while most of the BTIC samples still showed significant transfection. Fluorescence microscopy qualitatively confirmed these results (Figure 4D). The specificity of transfection at low doses has great implications for an *in vivo* application.

To determine if cell division rate was the determinant factor in the specificity of our polymers, we compared the cellular growth rates as well as the cellular uptake of nanoparticles in each primary culture of BTICs and fNPCs. Cellular growth rate can affect gene delivery, as the nuclear membrane is a significant delivery barrier preventing exogenous plasmid DNA from being able to be successfully transcribed. Cells that quickly divide quickly can reduce the impact of this barrier and increase the likelihood of successful transfection. There was no statistically significant difference between the cellular doubling times of BTICs and fNPCs, indicating cell division rate was not a factor in this observation (Figure S2, Supporting Information).

We then evaluated if particle uptake, an important step for particle-mediated intracellular gene delivery, was different between BTICs and fNPCs. There was no statistically significant difference between cellular uptake of nanoparticles in fNPCs compared to BTICs (Figure S2, Supporting Information). This result was

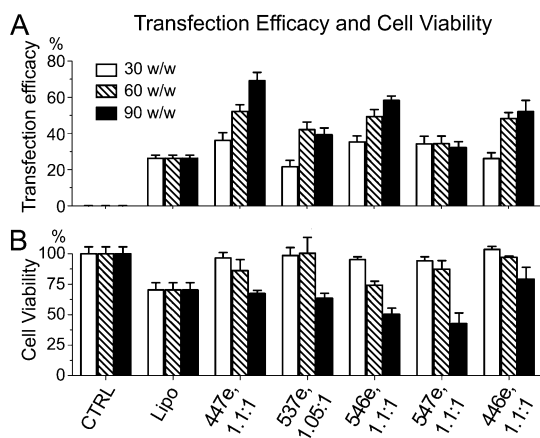


Figure 2. Transfection efficacy and safety of leading PBAE nanoparticles at transfecting human GBM BTIC oncospheres (primary JHGBM-551 cells). (A) Transfection efficacy was measured by percent of cells expressing DsRed. **(B)** Viability was measured by relative metabolic activity normalized to untreated cells. Polymer formulations are shown on the x-axes. CTRL: untreated control. Lipo: Lipofectamine 2000 control reagent. Bar graphs show mean \pm standard error of the mean (SEM).

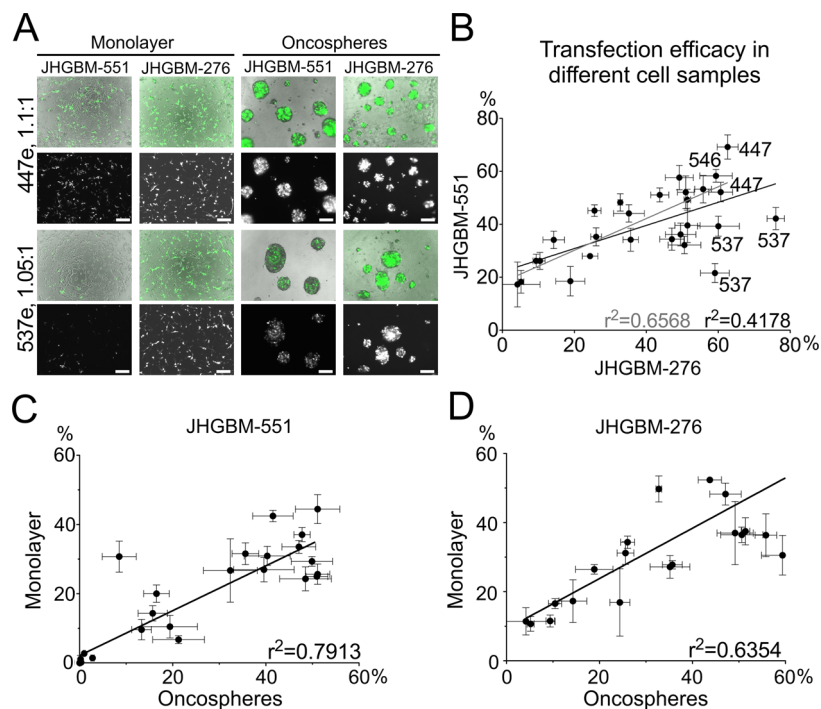


Figure 3. PBAE nanoparticles transfect BTIC oncospheres and monolayers from different patient sources. (A) Fluorescence and brightfield micrographs showing transfection of JHGBM-551 and JHGBM-276 primary cultures with PBAE 447e, effective for transfection of both cell types, and PBAE 537e, more effective for transfection of JHGBM-276 than JHGBM-551. In each pair of images, (top) brightfield and transgene signal merged (DsRed or GFP, false-colored green for both) and (bottom) DsRed or GFP only. **(B)** Correlation between transfection efficacy of all PBAEs and JHGBM-551 and JHGBM-276 oncospheres (black line) and for comparison without including outlier PBAE 537e (gray line). Points on the graph are labeled with the PBAE used to transfet them. **(C, D)** Transfection in 2-D (monolayer) and in 3-D (oncospheres) shows high correlation ($r^2 = 0.79, 0.64$). Graphs show mean \pm standard error of the mean (SEM).

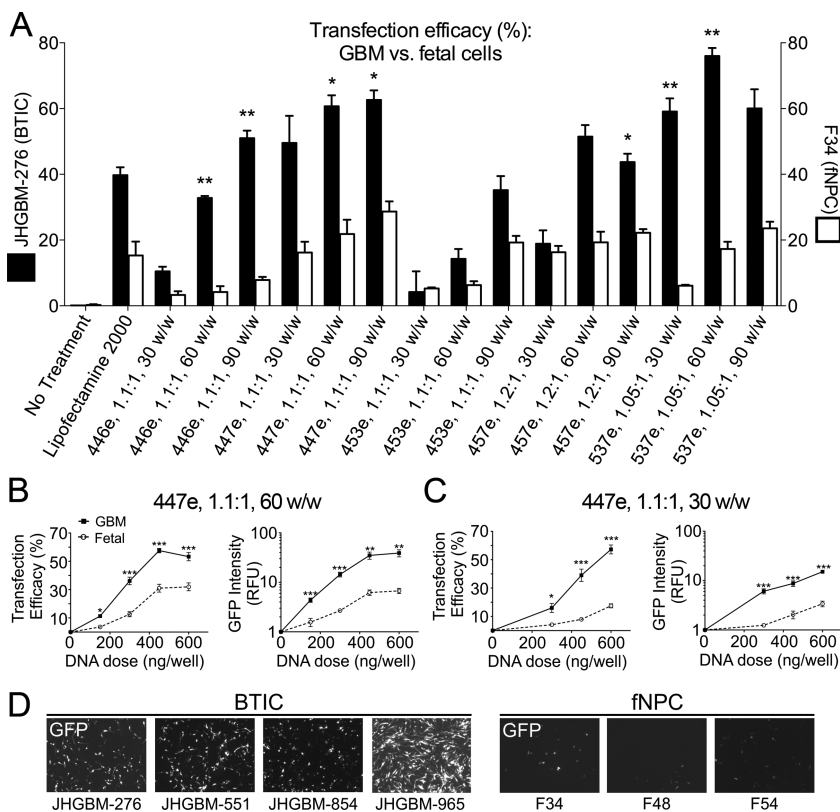


Figure 4. PBAE nanoparticles as GBM-specific gene delivery vehicles. JHGBM-276 BTICs and F34 fNPCs were transfected with leading PBAE formulations. (A) Several polymers showed a higher transfection efficacy in JHGBM-276s cells when compared with healthy cells. (B, C) BTICs were more efficiently transfected with top polymer (447e, tested at 30 and 60 w/w) than fNPCs at equivalent w/w ratios and nanoparticle doses, measured by percent of cells transfected and GFP fluorescence intensity. (D) Fluorescence micrographs qualitatively show the same result. For all graphs, * $p < 0.05$, ** $p < 0.01$, *** $p < 0.001$. Graphs show mean \pm standard error of the mean (SEM).

obtained both when measuring uptake as the percent of cells that are positive for uptake of particles containing fluorescently labeled DNA as well as by total relative fluorescence from uptake of these particles. Even though transfection efficacy was much higher in the BTICs than the fNPCs, the fNPCs had a slightly higher median measure of cellular uptake (relative fluorescence units) compared to the BTICs. These findings indicate that factors other than overall particle uptake and cell division rate are the major contributors to the increased transgene expression seen in BTICs cells compared to healthy fNPCs.

Lyophilized DNA/PBAE Nanoparticles Retain Full Function for at Least 2 Years in Storage. Long-term storage of nanoparticles is necessary to increase the translational potential of this method. In preparation for *in vivo* studies, we freeze-dried nanoparticles after formation to allow them to be stored stably as well as more easily concentrated for administration of high doses at low injection volume. Previous work using 447e showed that DNA/PBAE nanoparticles lyophilized with sucrose as a protectant retained full transfection efficacy after being stored for 3 months at 4 °C, although efficacy decreased to ~50% after 6 months of storage (Figure 5). To further determine the shelf life of PBAE nanoparticles, we evaluated lyophilization with different added

amounts of sucrose (0–45 mg/mL) and different storage conditions (room temperature ~25, 4, and –20 °C) over a time period of 2 years. While nanoparticles without added sucrose rapidly lost efficacy, nanoparticles formulated at 30 and 45 mg/mL sucrose maintained full efficacy for at least 2 years when stored at –20 °C (Figure 5).

Physical and Chemical Characteristics of Nanoparticles Are Conducive to Intracellular Delivery. The polymer 447e, 1:1:1 had a number-average molecular weight of 11.3 kDa and weight-average molecular weight of 36.8 kDa, measured by gel permeation chromatography (GPC). Nanoparticles were made by complexing 447e and DsRed DNA at 60 w/w, lyophilized with 30 mg/mL sucrose, and stored at –20 °C until use. After resuspending the particles in water, we characterized them by nanoparticle tracking analysis (NTA), which measured a mean number-weighted hydrodynamic diameter of 143 nm in PBS (44 nm standard deviation), and by dynamic light scattering, which measured a zeta potential of +16.4 mV (0.96 mV standard error of the mean of five measurements). We have recently shown successful *in vivo* ophthalmic gene delivery using lyophilized nanoparticles reconstituted at high concentration.³⁰ Here, we evaluated whether our frozen nanoparticles maintained *in vivo* transfection

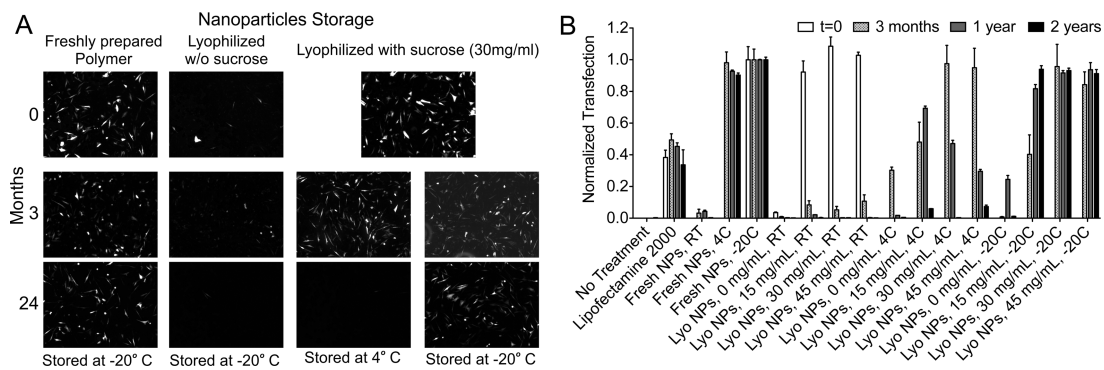


Figure 5. Efficacy of lyophilized nanoparticles after long-term storage. (A) Lyophilized nanoparticles of 447e and GFP DNA retained 100% efficacy after 2 years of storage at -20°C with 30 mg/mL or more of sucrose. Fluorescence micrographs show GFP signal from JHGBM-319 cells after transfection. (B) 447e/DNA nanoparticles retained 100% efficacy after lyophilization with 30 mg/mL or more of sucrose and storage at -20°C for at least 2 years, quantified by flow cytometry. Graphs show mean \pm standard error of the mean (SEM).

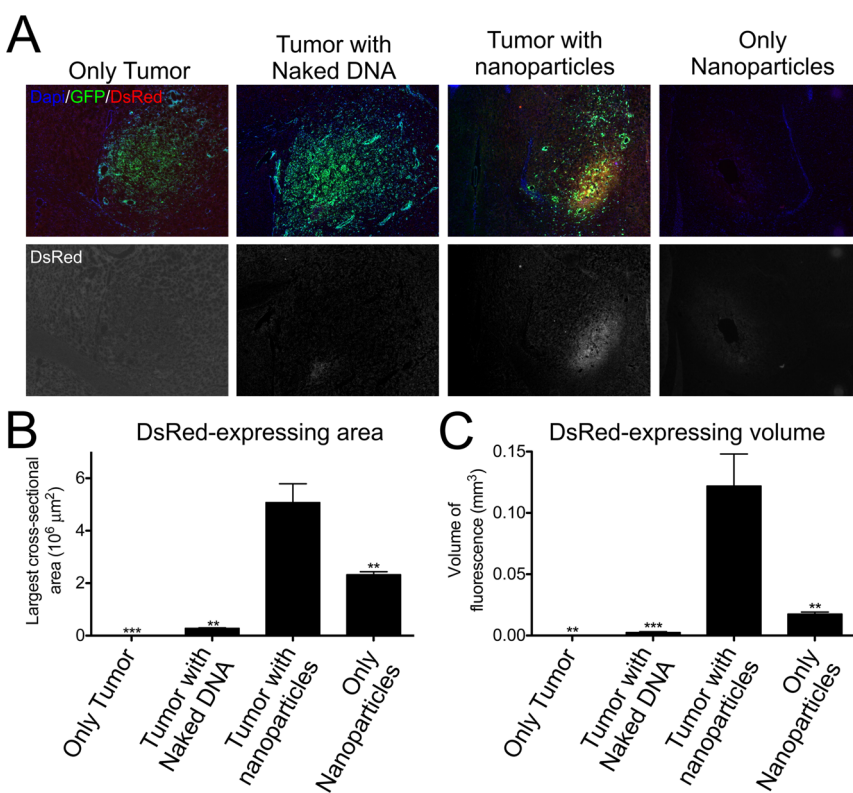


Figure 6. Transfection of human BTIC over healthy brain *in vivo*. (A) Microscope images showing the expression of DsRed and GFP in mice injected with either naked DNA or nanoparticles. (B–C) Significantly more transfection was seen in the 447e/DNA nanoparticle treatment group compared to the naked DNA group, as well as in the tumor group compared to the controls with nanoparticles but no tumor. ** $p < 0.01$, *** $p < 0.001$. Graphs show mean \pm standard error of the mean (SEM).

efficacy after reconstitution and evaluated efficacy in an orthotopic tumor model for the first time. We used 447e, 1.1;1, lyophilized, stored for 1–12 weeks at -20°C , and then reconstituted just prior to *in vivo* injection.

PBAE/DNA Nanoparticles Specifically Transfect Tumor Cells *in Vivo*. Orthotopic tumors formed from GFP-labeled human BTICs (JHGBM-276) in nude athymic mice were allowed to grow for 9 weeks. After tumor formation, lyophilized PBAE/DsRed-DNA particles (stored for 12 weeks) were reconstituted and immediately injected intratumorally. Assessment via fluorescence microscopy

showed that naked DNA caused very little expression. The expression level was drastically increased by using nanoparticles containing both DNA and 447e (Figure 6), quantified both by comparing the largest cross-sectional area of DsRed signal in each brain and by comparing the total volume of DsRed signal in each brain. Importantly, nanoparticles injected into tumors showed statistically significantly better transfection ($p < 0.01$) than nanoparticles injected into brain without tumor, similar to *in vitro* results that showed better transfection of BTICs compared to fetal (noncancer) fNPCs. This study also demonstrated the

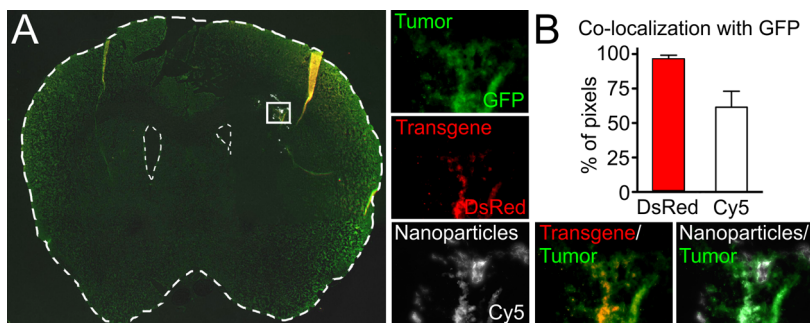


Figure 7. Tumor cell-specific transfection *in vivo*. (A) Coronal section of a tumor-bearing brain showing a small region containing tumor cells and nanoparticles (inset). Fluorescence microscopy shows distinct signals from GFP⁺ tumor cells, DsRed⁺ transfected cells, and Cy5⁺ nanoparticles. (B) Image-based colocalization analysis shows nearly 100% colocalization of transfected cells with tumor cells and <60% colocalization of nanoparticles with tumor cells. Graphs show mean \pm standard error of the mean (SEM).

translational potential of this technology as the lyophilized biodegradable nanoparticles used in this study had been stored for 3 months prior to use and worked well *in vivo* following simple reconstitution in PBS.

To further evaluate the nanoparticle specificity for tumor cells *in vivo*, colocalization analysis was performed on micrographs of mouse brains following Cy5-labeled DsRed nanoparticle injection into tumors formed over 4 weeks instead of 9 weeks. By allowing only 4 weeks for tumor growth, fluorescence (brain cancer constitutive GFP and/or DsRed exogenous expression) could be seen in individual cells more clearly (Figure 7), rather than by larger sections of tissue as was seen after 9 weeks (Figure 6). Using a method previously described,³¹ we used image analysis to calculate a normalized mean deviation product (nMDP) at each point of the images taken on both fluorescence channels as follows

$$\text{nMDP} = \frac{(I_{\text{GFP}} - I_{\text{GFP}, \text{avg}})(I_{\text{DsRed}} - I_{\text{DsRed}, \text{avg}})}{(I_{\text{GFP}, \text{max}} - I_{\text{GFP}, \text{avg}})(I_{\text{DsRed}, \text{max}} - I_{\text{DsRed}, \text{avg}})}$$

where I = intensity. Thus, an nMDP index between -1 and $+1$ was calculated for each point in the region of interest, with positive numbers corresponding to colocalization of the two fluorescence color signals and negative corresponding to lack of colocalization. nMDP indices between -0.1 and $+0.1$ were considered to represent autofluorescence and were excluded from consideration. Of the parts of the image that were DsRed⁺, more pixels were also positive for GFP than pixels negative for GFP. No points in the images had an nMDP index of <-0.5 for DsRed/GFP colocalization, while indices of $+0.5$ to $+1$ were found, and fewer than 5% of all DsRed⁺ pixels were found to be GFP⁻, indicating that the DsRed⁺ signal was far more likely to be in tumor cells than in healthy brain tissue. This *in vivo* finding clearly supports the *in vitro* finding that gene expression with these materials is highly specific to cancer cells over healthy cells. Interestingly, when the same analysis was performed on the Cy5/GFP signal, to detect the location of cellular uptake of nanoparticles, rather than detecting

only successfully transfected cells, a lower degree of colocalization was found. Although >50% of Cy5 signal was colocalized with GFP signal, which was expected as the Cy5⁺ nanoparticles were stereotactically injected into the same region as the tumor, >35% of Cy5⁺ pixels were found in nontumor tissue. Thus, like *in vitro*, while nanoparticles can be efficiently taken up by noncancer cells, they seem to only efficiently express the delivered transgene within cancer cells.

DISCUSSION

Our work demonstrates that PBAE nanoparticles can be used to specifically target brain cancer cells *in vitro* and *in vivo*. Our *in vitro* work shows that we can transfet BTICs not only in a monolayer culture but also in 3-D oncosphere culture. Aside from demonstrating the ability of PBAE nanoparticles to penetrate and transfet cells in 3-D, as in an *in vivo* environment, the high correlation between transfection of monolayer and oncosphere cultures also suggests that two-dimensional transfection studies, which are common initial experiments, have predictive value for the more clinically relevant three-dimensional case. Moreover, the correlation between two BTIC cultures (JHGBM-276 and JHGBM-551), each of which was derived from a different human GBM patient, suggest that the PBAEs identified here to be top candidates for transfection will also likely be effective on cells derived from other tumors from other GBM patients, although a more extensive study with more samples would be necessary to confirm this trend. A leading polymer in the JHGBM-276 sample, 537e, was found to be less effective in JHGBM-551 cells. This shows that there is potentially some patient-source specificity for certain polymers. The 447e polymer was chosen to be used for *in vivo* studies because it was a particularly effective polymer in all of the four primary BTIC samples tested.

While nonviral, nanoparticle-based delivery of drugs and nucleic acids have been a subject of much research, many hurdles must still be overcome for their use in an *in vivo* or clinical setting.^{32,33} Because surgical

intervention is common in GBM treatment, local application of therapeutic nanoparticles is a relevant strategy. However, even direct, local injection of nanoparticles is met with challenges in distribution and efficacy that can be overcome in particle design and chemical composition.^{34,35} Our finding in this study that cancer cells were specifically transfected with the nanoparticles over non-cancer cells supports previous work showing similar results in different settings.^{29,36} Interestingly, this finding was not due to factors such as cellular division rate, cellular uptake of nanoparticles, or media composition. While the exact mechanism for the nanoparticle-mediated cancer specificity remains elusive, it is dependent on polymer structure and polymer to DNA weight ratio (Figure 4A). We hypothesize that the differences in transfection may be the result of differential pathways of endocytosis (even though total endocytosis appears the same) and that these pathways may be cell-type dependent and tunable by differential polymer structures.³⁷ This is a subject of active investigation by our group. Nevertheless, we have observed this phenomenon consistently among many patient samples and both *in vitro* and *in vivo*.

For this nanoparticle technology to be translated to a clinical setting, a method for making nanoparticles in a more stable form is necessary. When prepared in aqueous solution, these nanoparticles self-assemble quickly but also aggregate over time. In addition, while there appears to be some slowing of polymer degradation when the PBAE polymers are complexed with DNA into particles,²¹ the PBAEs remain hydrolytically degradable. Therefore, it would be preferable to formulate the biodegradable nanoparticles in a form that is stable over time, resisting both degradation as well as aggregation. A concern is that many freezing and drying processes themselves cause denaturation or irreversible aggregation of nanoparticles. We have previously described the formulation of sucrose-protected lyophilized nanoparticles for *in vitro* and *in vivo* transfection and short-term storage; our data now show that the optimized lyophilized nanoparticles can be stored at -20°C and remain fully functional, as measured by *in vitro* efficacy, for at least two years. Furthermore, our *in vivo* studies validate that these stored nanoparticles remain efficacious *in vivo* following storage for at least 3 months. In addition to simplifying the preparation—essential for use in complicated surgical procedures—lyophilized PBAE/DNA complexes can be easily resuspended in water or PBS to almost any concentration, including concentrations

much higher than how they were originally prepared in aqueous buffer. We have found that this is because the solubility of the polymeric nanoparticles lyophilized with sucrose and resuspended in water is higher than the solubility of the uncomplexed polymer in water. This is an important consideration due to the small injection volume limitations for certain therapeutic applications such as injection into the eye or brain.

In the mouse GBM models, it was promising to see that these polymer-based, nonviral nanoparticles were able to transfect tumor cells upon injection using a polymer selected from an *in vitro* screen. Moreover, the PBAE nanoparticles exhibit selectivity for tumor cells over healthy cells *in vivo*. Although there remains the possibility that the selectivity observed *in vivo* is for human cells (tumor) over mouse cells (healthy brain), the results do corroborate the *in vitro* results showing selectivity for human BTICs over human fNPCs. Particularly telling is the result that the physical distribution of nanoparticles *in vivo* has a lower degree of colocalization with tumor cells than does the expression of the transgene. This indicates that while the nanoparticles may be convected or diffuse outside of the tumor space and enter healthy brain tissue cells, transgene expression will occur to a much lower extent in noncancer cells than in tumor cells. Although only a portion of the tumor was transfected in this study, it has already been shown that unmodified nanoparticles tend to have very limited diffusion within brain tissue.^{34,38} The ability of our particles to diffuse following a direct, local injection is comparable with other polymeric nanotechnologies studied in the brain, including nanoparticles specifically modified for increased diffusivity.³⁴ Because our PBAE-based nanoparticles can be used to deliver essentially any DNA sequence without changing the particles' physicochemical properties,²¹ they could, in future studies, be used to transfect a region of the tumor to express a secreted therapeutic protein that would subsequently diffuse away from the injection site to affect other regions of the tumor *via* a bystander effect.

CONCLUSIONS

This work introduces a nanobiotechnology with translational potential for treating glioblastoma, a disease in need of new therapies. With both *in vitro* and *in vivo* data showing high transfection and safety of the nanoparticles in human primary glioblastoma cells as well as intrinsic tumor cell specificity by the biomaterial, these materials are promising as vehicles for the deployment of anticancer genetic medicines.

MATERIALS AND METHODS

For details, see the Supporting Information

Materials. Lipofectamine 2000 (Invitrogen, Carlsbad, CA), Opti-MEM I (Invitrogen), pEGFP-N1 DNA (Elitz Biopharmaceuticals, Hayward, CA), pDsRed-Max-N1³⁹ (Addgene DNA plasmid

21718, Cambridge, MA), and cell culture media components were used as received. Monomers used for synthesizing polymers (Scheme 1) were purchased as follows: 1,3-butanediol diacrylate (B3b; Sigma-Aldrich, St. Louis, MO); 1,4-butanediol diacrylate (B4; Alfa Aesar, Ward Hill, MA); 1,5-pentanediol diacrylate (B5; Monomer-Polymer and Dajac Laboratories, Trevose,

PA); 3-amino-1-propanol (S3; Alfa Aesar); 4-amino-1-butanol (S4; Alfa Aesar); 5-amino-1-pentanol (S5; Alfa Aesar); 1,3-diaminopropane (E1; Sigma-Aldrich); 1,3-diaminopentane (E3; TCI America, Portland, OR); 2-methyl-1,5-diaminopentane (E4; TCI America); 1,11-diamino-3,6,9-trioxaundecane (E5; TCI America); 2-(3-aminopropylamino)ethanol (E6; Sigma-Aldrich); 1-(3-aminopropyl)-4-methylpiperazine (E7; Alfa Aesar); 1-(3-aminopropyl)pyrrolidine (E8; TCI America); and cystamine dihydrochloride (E10; Alfa Aesar). 4',6-Diamidino-2-phenylindole dihydrochloride (DAPI) was purchased from Sigma and used as a 750 nM solution in PBS. Other materials were reagent grade.

Polymer Synthesis. PBAEs were synthesized according to previously reported protocols.²¹ For initial screening, one diacrylate backbone ("B") monomer was mixed with one monoamino side chain ("S") monomer at a 1.2:1 molar ratio, with B in excess to ensure that the B–S base polymer would be diacrylate-terminated. The mixture was stirred at 90 °C for 24 h. The resulting base polymer was then dissolved in anhydrous dimethyl sulfoxide (DMSO). A 0.5-M solution of one end-cap ("E") small molecule in DMSO was added for a final base polymer concentration of 100 mg/mL, and the mixture was vortexed for 1 h at room temperature. Polymers were stored until use at 4 °C in small aliquots to reduce the number of freeze–thaw cycles.

Top polymers were chosen from the initial transfection screening done in JHGBM-551 BTICs. These polymers were resynthesized in a purified form as described previously at B:S ratios ranging from 1.05:1 to 1.2:1.³⁶ Briefly, the base polymer and end-cap were dissolved in anhydrous tetrahydrofuran (THF) instead of DMSO. After 1 h of stirring at room temperature, the polymers were precipitated into anhydrous diethyl ether. The precipitate was collected by centrifugation, washed again with ether, and centrifuged to isolate the end-capped polymer. Residual ether was removed under vacuum for 48 h. The dry PBAEs were then dissolved in anhydrous DMSO (100 mg/mL) and stored at –20 °C in small aliquots until use.

Molecular weight of the top polymer was measured by gel permeation chromatography (GPC; Waters, Milford, MA) in BHT-stabilized tetrahydrofuran with 5% DMSO and 1% piperidine. Number-averaged and weight-averaged molecular weight (M_n and M_w , respectively) were calculated using polystyrene standards.

Cell Culture. All the primary cultures of BTICs studied here were obtained from adult patients undergoing surgery for GBM (Table 1), after informed consent, following institutionally approved protocols. Samples were prepared and maintained as previously described.⁴⁰ Cells were maintained in culture as nonadherent oncospheres in complete BTIC medium [DMEM/F-12 (1:1) with 1X B-27 supplement, 1% antibiotic–antimycotic (Invitrogen), 20 ng/mL basic fibroblast growth factor (bFGF), and 20 ng/mL epidermal growth factor (EGF)]. For passaging, oncospheres were collected by centrifugation and were mechanically dissociated by titration. Primary cultures of human fetal neural progenitor cells (fNPCs) F34, F48, and F54 were obtained as described previously.^{29,41} Briefly, following approval by the Johns Hopkins University Institutional Review Board, intraoperative human central nervous system (CNS) tissues were obtained at 17 weeks of gestation, which were obtained following written informed consent for clinical procedures, were used for this research since they were considered to be pathological waste. Brain cortical tissue was mechanically dissociated and cells were maintained in 2:1 high-glucose DMEM (Invitrogen)/Ham's F-12 (Cellgro), 1X B-27, 1% anti–anti, 20 ng/mL bFGF, 20 ng/mL EGF, 20 ng/mL leukemia inhibitory factor (LIF, Millipore, Billerica, MA), and 5 µg/mL heparin (Sigma).

Preparation of Cy3-Labeled DNA. eGFP DNA was labeled with Cy3 using a Label IT Tracker kit (Mirus Bio) according to the manufacturer's instructions. Briefly, a solution of 125 µg/mL DNA and 100 µL/mL Label IT Tracker reagent was prepared in buffer and then incubated at 37 °C for 3 h on an orbital shaker. The labeled DNA was precipitated with ethanol in 300 mM sodium acetate buffer and cooled at –20 °C for 30 min. The DNA was pelleted by centrifugation at 15000g at 4 °C for 15 min, washed with 70% ethanol, and centrifuged again. The dried pellet was reconstituted in fresh unlabeled eGFP DNA in water. The concentration was verified using absorbance at 260 nm using a Nanodrop 2000 with associated software (v. 1.4.1)

TABLE 1. Primary Cultures Used

name	cell type	source
JHGBM-276	GBM (BTIC)	53-y.o. patient
JHGBM-319	GBM	79-y.o. patient
JHGBM-551	GBM (BTIC)	69-y.o. patient
JHGBM-854	GBM (BTIC)	41-y.o. patient
JHGBM-965	GBM (BTIC)	61-y.o. patient
F34	fNPC	17 gestational wk
F48	fNPC	17 gestational wk
F54	fNPC	17 gestational wk

(Thermo Fisher, Waltham, MA). The absence of protein from the solution was measured by absorbance at 280 nm ($A_{260}/A_{280} \geq 1.7$). The labeled DNA was diluted further with unlabeled nucleic acid to a final dye-to-nucleotide molar ratio of 1:350.

Transfection Experiments *in Vitro*. For 3-D transfections, BTIC oncospheres 200–1000 µm in diameter were collected by centrifugation and resuspended in complete BTIC medium without dissociation using a 5 mL serological pipet. A small aliquot was removed, mechanically dissociated with a 200 µL micropipet, and used for counting and determination of cell density. Cells were seeded into round-bottom, nontissue culture-treated 96-well plates at 1.5×10^4 cells/well in 100 µL complete culture medium and incubated at 37 °C overnight.

For nanoparticle preparation, DsRed (for GFP⁺ JHGBM-551 cells) or eGFP DNA (for all other unlabeled cells) was diluted to 60 µg/mL in 25 mM sodium acetate pH 5 buffer (NaAc). PBAEs were diluted from their stock solutions in DMSO in 25 mM NaAc and added to DNA solutions at PBAE/DNA mass ratios (w/w) of 30, 60, or 90. The resulting mixture was mixed by pipetting and incubated at room temperature for 10 min to allow nanoparticles to form. Nanoparticles (20 µL) in NaAc were added directly to the oncospheres in culture medium in 96-well plates (final nanoparticle/medium ratio of 1:5, final DNA concentration of 5 µg/mL or 600 ng/well, final polymer concentration of 150–450 µg/mL). Oncospheres were incubated with particles at 37 °C for 2 h. A replicate of each plate was transfected in the same way for viability measurements. The plates were then centrifuged at 180g for 5 min. The media and remaining nanoparticles were removed and the oncospheres gently resuspended in complete culture medium. Viability was defined as the metabolic activity retained in each well following transfection, measured after 24 h by MTS (Cell Titer AQueousONE, Promega, Madison, WI) according to the manufacturer's instructions. Transfection efficacy was measured by fluorescence microscopy and by flow cytometry after 48 h using an Accuri C6 with a Hypercyt high-throughput robotic sampler (Intellicyt) after mechanically dissociating the oncospheres to single-cell suspensions. Transfection data were analyzed with FlowJo 7 software (Treestar). Experiments were done with $n = 4$ replicates.

After initial screening on JHGBM-551 oncospheres, purified polymers were used for all further experiments. Following a transfection screening using purified polymers, one optimized B/S synthesis ratio was chosen for each PBAE based on high transfection (percent of cells positive for transgene) and low loss in metabolic activity (MTS assay).

For 2-D transfections, a similar protocol was used. Flat-bottom, tissue-culture-treated 96-well plates were coated with 20 µg/mL laminin (Sigma) by incubation at room temperature for 1 h and then washing once with 1xPBS with Ca²⁺ and Mg²⁺. Oncospheres were collected by centrifugation, and the whole pellet was mechanically dissociated with a 200 µL pipet. Dissociated cells were then seeded at 1.5×10^4 cells/well in 100 µL of complete medium into laminin-coated plates. Cells were incubated overnight at 37 °C. For fNPCs, medium was replaced with complete BTIC medium immediately before transfection to ensure that any media interactions with nanoparticles were comparable for all the primary cultures tested. After transfection with DNA/PBAE nanoparticles and incubation for 2 h, the medium and nanoparticles were removed and replaced with fresh BTIC or fNPC culture medium. Viability and transfection

measurements were taken in the same way. For flow cytometry, cells were first trypsinized, resuspended in PBS with 2% FBS, and transferred to round-bottom 96-well plates for use with the Hypercyt reader.

Comparison of Fetal and GBM Cell Behavior *In Vitro*. Uptake of DNA-containing nanoparticles by fNPCs and BTICs was compared. Transfections were then carried out as above on monolayer cultures using fluorescently labeled DNA, keeping cells out of direct light to avoid photobleaching. Uptake was measured by flow cytometry immediately after 2 h of incubation with labeled nanoparticles.

To measure growth rate, BTICs or fNPCs were seeded into laminin-coated 96-well plates at 5000 cells/well and allowed to adhere overnight. At set time points, the metabolic activity of a set of wells was measured by MTS assay (Cell Titer). The doubling time for each BTIC and fNPC culture was calculated by fitting the data to an exponential growth curve.

Formulation and Testing of Lyophilized DNA Nanoparticles. To test the stability of lyophilized particles over time, eGFP DNA was complexed with 447e, 1.2:1, as described previously.²⁹ Briefly, plasmid DNA and 447e were mixed in 25 mM NaAc at a PBAE:DNA ratio of 30 w/w. After particle formation, a solution of d-sucrose in 25 mM NaAc was added for a final DNA concentration of 15 µg/mL and final sucrose concentration of 0, 15, 30, or 45 mg/mL. Nanoparticles were freeze-dried and stored at room temperature (rt), 4 °C, or –20 °C in small aliquots for up to 2 years.

To test the efficacy of stored nanoparticles at various time points, GBM cells (sample JHGBM-319) were seeded in 24-well plates in complete astrocyte medium at 7.5×10^4 cells/well in 500 µL volume. The cells were left overnight to adhere. The next day, nanoparticles were taken from storage and were resuspended in sterile water by pipetting to a final DNA concentration of 15 µg/mL. At the same time, fresh nanoparticles were prepared; briefly, fresh eGFP DNA was diluted in 25 mM NaAc at 30 µg/mL. PBAE 447e, stored in small aliquots at room temperature, 4 °C, or –20 °C, was dissolved in 25 mM NaAc and added to the DNA solution at 30 w/w for final DNA concentration of 15 µg/mL. Of reconstituted lyophilized or fresh nanoparticles (100 µL) were then added dropwise to 500 µL of complete astrocyte medium in each well (1.5 µg DNA/well). After 2 h incubation at 37 °C, media and nanoparticles were aspirated from each well and replaced with fresh complete astrocyte medium. Viability and transfection efficacy were measured by MTS assay and flow cytometry as described above and by fluorescence microscopy as described previously.²⁹

Nanoparticle Physicochemical Analysis. The top lyophilized particle formulation was sized using nanoparticle tracking analysis (NTA) using an NS500 (NanoSight, Ltd.). The zeta potential was measured using a Zetasizer Nano NS (Malvern). For both, nanoparticles were formed in 25 mM NaAc at the same concentration as used for transfections, then diluted in 1xPBS as necessary for sizing purposes.

In Vivo Testing of DNA Nanoparticles. Male nude athymic mice were injected with 1 µL of GFP⁺ JHGBM-276 cells in PBS (10^5 cells/µL) at 8 weeks old. After a 4- or 9-week period for tumor formation, nanoparticles composed of DsRed plasmid DNA complexed with 447e, 1.1:1, at 60 w/w, lyophilized with 30 mg/mL sucrose, and stored at –20 °C were resuspended in water. For particle localization studies, DsRed-coding DNA was first labeled with Cy5 using a Label IT Tracker kit (Mirus Bio) before complexation with PBAE. Nanoparticles (2 µL, 2 µg DNA) were stereotactically injected into the tumor of the mice. Controls included mice injected with nanoparticles but without tumor, mice with tumor but no treatment, and mice with tumor and injected with 2 µg naked DNA in a sucrose solution of the same concentration. After 48 h, mice were anaesthetized with ketamine/xylazine, sacrificed, and fixed by perfusion with PBS and 10% formalin. Brains were removed, stored overnight in 10% formalin, soaked in 30% sucrose in 1 × phosphate buffer for 24 h, and then embedded in Optimal cutting temperature compound (OCT). Embedded brains were snap frozen in a dry ice/ethanol bath and stored at –80 °C until use. Brains were cryosectioned in 10-µm slices and mounted onto glass slides

with DAPI and stored at 4 °C, protected from light, until use. Slices were imaged by fluorescence microscopy to assess transfection using an Axio Observer A1 and captured with Axiovision software.

Image Analysis of Brain Sections. The degree of transfection was assessed by image analysis. For mice with tumors that developed over 9 weeks, ImageJ was used to find the area of DsRed fluorescence in each section. ImageJ is a public domain program and was downloaded from <http://imagej.nih.gov/ij/>. The volume of transgene expression was estimated by multiplying the area of DsRed signal on each slice by the thickness of the slice and adding the resulting volumes. For mice with tumors that developed over only 4 weeks, the Colocalization Colormap plugin on ImageJ was used to find the degree of colocalization of the DsRed and GFP signals based on the method described in Jaskolski *et al.*³¹ The number of DsRed⁺ pixels that were colocalized with GFP signal was compared with DsRed⁺ pixels not colocalized with GFP. The same analysis was also carried out with Cy5 and GFP signal to compare pixels positive on both channels to pixels positive for Cy5 but not for GFP.

Statistical Analysis. Unless otherwise stated, bar graphs show mean ± standard error of the mean (SEM). Correlations between cell samples was determined using linear regression, with outliers defined as points with externally studentized residuals whose absolute values exceeded 2.5. Analysis was done with Prism software (Graphpad).

For comparisons between GBM (JHGBM-276, JHGBM-551, JHGBM-854, and JHGBM-965) and fetal cells (F34, F48, and F54), results from all cell sources were pooled to form a single cancer group and a single noncancer group. Comparisons were done at each transfection condition using a two-tailed Student's *t* test with a Bonferroni correction for multiple comparisons. Polymer transfection screens were analyzed via one-way ANOVA with a post hoc Dunnett test to determine statistical significance.

Conflict of Interest: The authors declare no competing financial interest.

Supporting Information Available: Data showing screening and optimization of PBAE nanoparticles for BTIC transfection and data on the mechanism of cancer specificity. This material is available free of charge via the Internet at <http://pubs.acs.org>.

Acknowledgment. This work was supported in part by the National Institutes of Health (1R01EB016721 and R21CA152473) and MSCRF-TEDCO. We thank Xiaobu Ye for help with statistical analysis. S.Y.T. thanks the National Science Foundation for fellowship support.

REFERENCES AND NOTES

- Porter, K. R.; McCarthy, B. J.; Freels, S.; Kim, Y.; Davis, F. G. Prevalence Estimates for Primary Brain Tumors in the United States by Age, Gender, Behavior, and Histology. *Neuro-Oncology* **2010**, *12*, 520–527.
- McGirt, M. J.; Chaichana, K. L.; Gathinji, M.; Attenello, F. J.; Than, K.; Olivi, A.; Weingart, J. D.; Brem, H.; Quinones-Hinojosa, A. R. Independent Association of Extent of Resection with Survival in Patients with Malignant Brain Astrocytoma. *J. Neurosurg.* **2009**, *110*, 156–162.
- McGirt, M. J.; Mukherjee, D.; Chaichana, K. L.; Than, K. D.; Weingart, J. D.; Quinones-Hinojosa, A. Association of Surgically Acquired Motor and Language Deficits on Overall Survival after Resection of Glioblastoma Multiforme. *Neurosurgery* **2009**, *65*, 463–469discussion 469–470.
- McGirt, M. J.; Than, K. D.; Weingart, J. D.; Chaichana, K. L.; Attenello, F. J.; Olivi, A.; Laterra, J.; Kleinberg, L. R.; Grossman, S. A.; Brem, H.; *et al.* Gliadel (Bcnu) Wafer Plus Concomitant Temozolomide Therapy after Primary Resection of Glioblastoma Multiforme. *J. Neurosurg.* **2009**, *110*, 583–588.
- Stupp, R.; Mason, W. P.; van den Bent, M. J.; Weller, M.; Fisher, B.; Taphoorn, M. J.; Belanger, K.; Brandes, A. A.; Marosi, C.; Bogdahn, U.; *et al.* Radiotherapy Plus Concomitant and Adjuvant Temozolomide for Glioblastoma. *N. Engl. J. Med.* **2005**, *352*, 987–996.

6. Chaichana, K. L.; Zadnik, P.; Weingart, J. D.; Olivi, A.; Gallia, G. L.; Blakeley, J.; Lim, M.; Brem, H.; Quinones-Hinojosa, A. Multiple Resections for Patients with Glioblastoma: Prolonging Survival. *J. Neurosurg.* **2013**, *118*, 812–820.
7. Chaichana, K. L.; Zaidi, H.; Pendleton, C.; McGirt, M. J.; Grossman, R.; Weingart, J. D.; Olivi, A.; Quinones-Hinojosa, A.; Brem, H. The Efficacy of Carmustine Wafers for Older Patients with Glioblastoma Multiforme: Prolonging Survival. *Neurol. Res.* **2011**, *33*, 759–764.
8. King, G. D.; Muhammad, A. K. M. G.; Larocque, D.; Kelson, K. R.; Xiong, W. D.; Liu, C. Y.; Sanderson, N. S. R.; Kroeger, K. M.; Castro, M. G.; Lowenstein, P. R. Combined Flt3/Tk Gene Therapy Induces Immunological Surveillance Which Mediates an Immune Response against a Surrogate Brain Tumor Neoantigen. *Mol. Ther.* **2011**, *19*, 1793–1801.
9. Chiocca, E. A.; Abbed, K. M.; Tatter, S.; Louis, D. N.; Hochberg, F. H.; Barker, F.; Kracher, J.; Grossman, S. A.; Fisher, J. D.; Carson, K.; et al. A Phase I Open-Label, Dose-Escalation, Multi-Institutional Trial of Injection with an E1b-Attenuated Adenovirus, Onyx-015, into the Peritumoral Region of Recurrent Malignant Gliomas, in the Adjuvant Setting. *Mol. Ther.* **2004**, *10*, 958–966.
10. Tai, C. K.; Wang, W. J.; Chen, T. C.; Kasahara, N. Single-Shot, Multicycle Suicide Gene Therapy by Replication-Competent Retrovirus Vectors Achieves Long-Term Survival Benefit in Experimental Glioma. *Mol. Ther.* **2005**, *12*, 842–851.
11. Bogler, O.; Huang, H. J. S.; Kleihues, P.; Cavenee, W. K. The P53 Gene and Its Role in Human Brain-Tumors. *Glia* **1995**, *15*, 308–327.
12. Tolcher, A. W.; Hao, D.; de Bono, J.; Miller, A.; Patnaik, A.; Hammond, L. A.; Smetzer, L.; Hood, J. V.; Merritt, J.; Rowinsky, E. K.; et al. Phase 1, Pharmacokinetic, and Pharmacodynamic Study of Intravenously Administered Ad5cmv-P53, an Adenoviral Vector Containing the Wild-Type P53 Gene, in Patients with Advanced Cancer. *J. Clin. Oncol.* **2006**, *24*, 2052–2058.
13. Lang, F. F.; Bruner, J. M.; Fuller, G. N.; Aldape, K.; Prados, M. D.; Chang, S.; Berger, M. S.; McDermott, M. W.; Kunwar, S. M.; Junck, L. R.; et al. Phase I Trial of Adenovirus-Mediated P53 Gene Therapy for Recurrent Glioma: Biological and Clinical Results. *J. Clin. Oncol.* **2003**, *21*, 2508–2518.
14. Tobias, A.; Ahmed, A.; Moon, K. S.; Lesniak, M. S. The Art of Gene Therapy for Glioma: A Review of the Challenging Road to the Bedside. *J. Neurol., Neurosurg., Psychiatry* **2013**, *84*, 213–222.
15. Chiocca, E. A.; Aghi, M.; Fulci, G. Viral Therapy for Glioblastoma. *Cancer J.* **2003**, *9*, 167–179.
16. Goodman, J. C.; Trask, T. W.; Chen, S. H.; Woo, S. L. C.; Grossman, R. G.; Carey, K. D.; Hubbard, G. B.; Carrier, D. A.; Rajagopalan, S.; AguilarCordova, E.; et al. Adenoviral-Mediated Thymidine Kinase Gene Transfer into the Primate Brain Followed by Systemic Ganciclovir: Pathologic, Radiologic, and Molecular Studies. *Hum. Gene Ther.* **1996**, *7*, 1241–1250.
17. Rainov, N. G.; Grp, G. I. S. A Phase III Clinical Evaluation of Herpes Simplex Virus Type 1 Thymidine Kinase and Ganciclovir Gene Therapy as an Adjuvant to Surgical Resection and Radiation in Adults with Previously Untreated Glioblastoma Multiforme. *Hum. Gene Ther.* **2000**, *11*, 2389–2401.
18. Kanasty, R.; Dorkin, J. R.; Vegas, A.; Anderson, D. Delivery Materials for siRNA Therapeutics. *Nat. Mater.* **2013**, *12*, 967–977.
19. Scholz, C.; Wagner, E. Therapeutic Plasmid DNA Versus siRNA Delivery: Common and Different Tasks for Synthetic Carriers. *J. Controlled Release* **2012**, *161*, 554–565.
20. Pack, D. W.; Hoffman, A. S.; Pun, S.; Stayton, P. S. Design and Development of Polymers for Gene Delivery. *Nat. Rev. Drug Discov.* **2005**, *4*, 581–593.
21. Tzeng, S. Y.; Green, J. J. Subtle Changes to Polymer Structure and Degradation Mechanism Enable Highly Effective Nanoparticles for siRNA and DNA Delivery to Human Brain Cancer. *Adv. Healthcare Mater.* **2013**, *2*, 468–480.
22. Bishop, C. J.; Ketola, T. M.; Tzeng, S. Y.; Sunshine, J. C.; Urtti, A.; Lemmetyinen, H.; Vuorimaa-Laukkonen, E.; Yliperttula, M.; Green, J. J. The Effect and Role of Carbon Atoms in Poly(Beta-Amino Ester)S for DNA Binding and Gene Delivery. *J. Am. Chem. Soc.* **2013**, *135*, 6951–6957.
23. Sunshine, J. C.; Akanda, M. I.; Li, D.; Kozielski, K. L.; Green, J. J. Effects of Base Polymer Hydrophobicity and End-Group Modification on Polymeric Gene Delivery. *Biomacromolecules* **2011**, *12*, 3592–3600.
24. Bhise, N. S.; Shmueli, R. B.; Gonzalez, J.; Green, J. J. A Novel Assay for Quantifying the Number of Plasmids Encapsulated by Polymer Nanoparticles. *Small* **2012**, *8*, 367–373.
25. Sunshine, J. C.; Peng, D. Y.; Green, J. J. Uptake and Transfection with Polymeric Nanoparticles Are Dependent on Polymer End-Group Structure, but Largely Independent of Nanoparticle Physical and Chemical Properties. *Mol. Pharm.* **2012**, *9*, 3375–3383.
26. Kamat, C. D.; Shmueli, R. B.; Connis, N.; Rudin, C. M.; Green, J. J.; Hann, C. L. Poly(Beta-Amino Ester) Nanoparticle Delivery of Tp53 Has Activity against Small Cell Lung Cancer *in Vitro* and *in Vivo*. *Mol. Cancer Ther.* **2013**, *12*, 405–415.
27. Davis, M. E.; Zuckerman, J. E.; Choi, C. H.; Seligson, D.; Tolcher, A.; Alabi, C. A.; Yen, Y.; Heidel, J. D.; Ribas, A. Evidence of RNAi in Humans from Systemically Administered siRNA via Targeted Nanoparticles. *Nature* **2010**, *464*, 1067–1070.
28. Huang, Y. H.; Zugates, G. T.; Peng, W.; Holtz, D.; Dunton, C.; Green, J. J.; Hossain, N.; Chernick, M. R.; Padera, R. F., Jr.; Langer, R.; et al. Nanoparticle-Delivered Suicide Gene Therapy Effectively Reduces Ovarian Tumor Burden in Mice. *Cancer Res.* **2009**, *69*, 6184–6191.
29. Tzeng, S. Y.; Guerrero-Cazares, H.; Martinez, E. E.; Sunshine, J. C.; Quinones-Hinojosa, A.; Green, J. J. Non-Viral Gene Delivery Nanoparticles Based on Poly(Beta-Amino Esters) for Treatment of Glioblastoma. *Biomaterials* **2011**, *32*, 5402–5410.
30. Sunshine, J. C.; Sunshine, S. B.; Bhutto, I.; Handa, J. T.; Green, J. J. Poly(Beta-Amino Ester)-Nanoparticle Mediated Transfection of Retinal Pigment Epithelial Cells *in Vitro* and *in Vivo*. *PLoS One* **2012**, *7*, 123–129.
31. Jaskolski, F.; Mulle, C.; Manzoni, O. J. An Automated Method to Quantify and Visualize Colocalized Fluorescent Signals. *J. Neurosci Methods* **2005**, *146*, 42–49.
32. Zuckerman, J. E.; Choi, C. H. J.; Han, H.; Davis, M. E. Polycation-siRNA Nanoparticles Can Disassemble at the Kidney Glomerular Basement Membrane. *Proc. Natl. Acad. Sci. U.S.A.* **2012**, *109*, 3137–3142.
33. Zhang, Y.; Satterlee, A.; Huang, L. *In Vivo* Gene Delivery by Nonviral Vectors: Overcoming Hurdles? *Mol. Ther.* **2012**, *20*, 1298–1304.
34. Nance, E. A.; Woodworth, G. F.; Sailor, K. A.; Shih, T. Y.; Xu, Q. G.; Swaminathan, G.; Xiang, D.; Eberhart, C.; Hanes, J. A Dense Poly(ethylene glycol) Coating Improves Penetration of Large Polymeric Nanoparticles within Brain Tissue. *Sci. Transl Med.* **2012**, *4*.
35. Jiang, Q. Y.; Lai, L. H.; Shen, J.; Wang, Q. Q.; Xu, F. J.; Tang, G. P. Gene Delivery to Tumor Cells by Cationic Polymeric Nanovectors Coupled to Folic Acid and the Cell-Penetrating Peptide Octaarginine. *Biomaterials* **2011**, *32*, 7253–7262.
36. Tzeng, S. Y.; Higgins, L. J.; Pomper, M. G.; Green, J. J. Biomaterial-Mediated Cancer-Specific DNA Delivery to Liver Cell Cultures Using Synthetic Poly(β -amino ester)s. *J. Biomed Mater. Res. A* **2013**, *101*, 1837–1845(Student Award Winner in the Ph.D. Category for the 2013 Society for Biomaterials Annual Meeting and Exposition, Apr 10–13, 2013, Boston, MA).
37. Kim, J.; Sunshine, J. C.; Green, J. J. Differential Polymer Structure Tunes Mechanism of Cellular Uptake and Transfection Routes of Poly(β -amino ester) Polyplexes in Human Breast Cancer Cells. *Bioconjugate Chem.* **2014**, *25*, 43–51.
38. Thorne, R. G.; Nicholson, C. *In Vivo* Diffusion Analysis with Quantum Dots and Dextrans Predicts the Width of Brain Extracellular Space. *Proc. Natl. Acad. Sci. U.S.A.* **2006**, *103*, 5567–5572.

39. Strack, R. L.; Strongin, D. E.; Bhattacharyya, D.; Tao, W.; Berman, A.; Broxmeyer, H. E.; Keenan, R. J.; Glick, B. S. A Noncytotoxic Dsred Variant for Whole-Cell Labeling. *Nat. Methods* **2008**, *5*, 955–957.
40. Guerrero-Cazares, H.; Chaichana, K. L.; Quinones-Hinojosa, A. Neurosphere Culture and Human Organotypic Model to Evaluate Brain Tumor Stem Cells. *Methods Mol. Biol.* **2009**, *568*, 73–83.
41. Ravin, R.; Blank, P. S.; Steinkamp, A.; Rappaport, S. M.; Ravin, N.; Bezrukova, L.; Guerrero-Cazares, H.; Quinones-Hinojosa, A.; Bezrukova, S. M.; Zimmerberg, J. Shear Forces During Blast, Not Abrupt Changes in Pressure Alone, Generate Calcium Activity in Human Brain Cells. *PLoS One* **2012**, *7*, e39421.